The Plant Cell, Vol. 29: 2269–2284, September 2017, www.plantcell.org © 2017 ASPB.

Light and Ethylene Coordinately Regulate the Phosphate Starvation Response through Transcriptional Regulation of *PHOSPHATE STARVATION RESPONSE1*

Yang Liu,[a,1] Yurong Xie,[a,1] Hai Wang,[a] Xiaojing Ma,[a] Wenjun Yao,[a] and Haiyang Wang[a,b,c,2]

[a] Biotechnology Research Institute, Chinese Academy of Agricultural Sciences, Beijing 100081, China
[b] State Key Laboratory for Conservation and Utilization of Subtropical Agro-Bioresources, Guangzhou 510642, China
[c] College of Life Sciences, South China Agricultural University, Guangzhou 510642, China

ORCID ID: 0000-0002-1302-5747 (H.Y.W.)

Plants have evolved an array of adaptive responses to low Pi availability, a process modulated by various external stimuli and endogenous growth regulatory signals. Little is known about how these signaling processes interact to produce an integrated response. *Arabidopsis thaliana PHOSPHATE STARVATION RESPONSE1* (*PHR1*) encodes a conserved MYB-type transcription factor that is essential for programming Pi starvation-induced gene expression and downstream Pi starvation responses (PSRs). Here, we show that loss-of-function mutations in *FHY3* and *FAR1*, encoding two positive regulators of phytochrome signaling, and in *EIN3*, encoding a master regulator of ethylene responses, cause attenuated *PHR1* expression, whereas mutation in *HY5*, encoding another positive regulator of light signaling, causes increased *PHR1* expression. FHY3, FAR1, HY5, and EIN3 directly bind to the *PHR1* promoter through distinct *cis*-elements. FHY3, FAR1, and EIN3 activate, while HY5 represses, *PHR1* expression. FHY3 directly interacts with EIN3, and HY5 suppresses the transcriptional activation activity of FHY3 and EIN3 on *PHR1*. Finally, both light and ethylene promote FHY3 protein accumulation, and ethylene blocks the light-promoted stabilization of HY5. Our results suggest that light and ethylene coordinately regulate *PHR1* expression and PSRs through signaling convergence at the *PHR1* promoter.

INTRODUCTION

Phosphorus (P) is an essential macronutrient for plant growth, development, and metabolism. Although P is abundant in most soils, Pi, the major form of P that plants assimilate, is highly immobile in most soils and, thus, P is one of the most limiting nutrients for crop productivity (Raghothama, 1999). To cope with Pi deficiency, plants have evolved an array of adaptive responses to remobilize internal Pi for redistribution and to enhance external Pi acquisition. Phosphate starvation responses (PSRs) include the remodeling of root system architecture (RSA) (cessation of primary root growth and increased proliferation of root hairs and lateral roots), reduced photosynthesis, enhanced high-affinity Pi transporter activity, and the accumulation of anthocyanin pigments and starch (López-Arredondo et al., 2014).

Much effort has been devoted to dissecting the Pi signaling mechanisms in plants. Local sensing of low Pi in the rhizosphere by a root-localized mechanism is thought to cause major root developmental changes better suited for enhancing Pi acquisition, whereas long-distance or systemic sensing triggers changes in the expression of numerous genes involved in Pi transport and distribution (Chiou and Lin, 2011; Zhang et al., 2014). The exact mechanisms underlying extracellular sensing of Pi have remained unclear; however, several key factors (e.g., *PHOSPHATE STARVATION RESPONSE1* [*PHR1*], *microRNA399* [*MIR399*], *PHOSPHATE1* [*PHO1*], and *PHO2*) involved in Pi systemic signaling have been identified and functionally characterized in several plant species (Poirier et al., 1991; Delhaize and Randall, 1995; Rubio et al., 2001; Bari et al., 2006). Among these, *Arabidopsis thaliana PHR1*, a homolog of *PSR1* (*PHOSPHORUS STARVATION RESPONSE1*) in *Chlamydomonas reinhardtii*, is the best studied to date. *PHR1* encodes a conserved MYB-type transcription factor that plays a crucial role in regulating most PSRs via transcriptional regulation of phosphate starvation-induced (PSI) genes, including genes involved in Pi transport and remobilization, anthocyanin biosynthesis, carbohydrate metabolism, and remodeling of RSA (Rubio et al., 2001; Nilsson et al., 2007; Bustos et al., 2010). PHR1 and its close homolog PHL1 (PHR1-Like1) directly bind to the *cis*-element P1BS (Rubio et al., 2001), which is prevalent in the promoters of many PSI genes, including *PHO1*, *MIR399*, *IPS1* (*INDUCED BY PHOSPHATE STARVATION1*), and *RNS1* (*RIBONUCLEASE1*) (Poirier et al., 1991; Bariola et al., 1994; Martín et al., 2000; Bari et al., 2006). Previous studies have revealed multiple mechanisms regulating PHR1 activity at the posttranscriptional levels. SPX1, a nucleus-localized SYG/PHO81/XPR1 domain protein, sequesters PHR1 in a Pi-dependent manner and inhibits its activity (Puga et al., 2014). Arabidopsis PHR1 can also be sumoylated in vitro by SIZ1, a SUMO E3 ligase (Miura et al., 2005). Intriguingly, the transcript level of *PHR1* is only weakly responsive to Pi deprivation stress, and the mechanism underlying its transcriptional regulation has remained largely unknown (Rubio et al., 2001).

[1] These authors contributed equally to this work.
[2] Address correspondence to wanghaiyang@caas.cn.
The author responsible for distribution of materials integral to the findings presented in this article in accordance with the policy described in the Instructions for Authors (www.plantcell.org) is: Haiyang Wang (wanghaiyang@caas.cn).
www.plantcell.org/cgi/doi/10.1105/tpc.17.00268

Pi signaling and PSRs are modulated by various internal and external factors, including light, sugar, various phytohormones (auxin, ethylene, cytokinins, and gibberellins), and oxygen deficiency stress (Jiang et al., 2007; Karthikeyan et al., 2007; Lei et al., 2011b; Klecker et al., 2014). Light, one of the most important dynamic environmental factors, not only provides energy through incident photosynthesis but also serves as an information signal to control plant growth and development (Chen et al., 2004). Substantial evidence has accumulated that active photosynthesis or sugars are required for PSRs and the expression of PSI genes under Pi-limiting conditions in Arabidopsis and several other plant species (Liu et al., 2005, 2010; Jain et al., 2007; Karthikeyan et al., 2007; Lei et al., 2011a). For example, Karthikeyan et al. (2007) found that the expression of PSI genes is greatly reduced in dark-grown plants, and this reduction is restored by adding sucrose to the growth medium. Similarly, exogenous application of sucrose stimulates the expression of *PT1* (a Pi transporter gene), *SAP1* (an APase gene), and *MIR399* in dark-grown white lupin (*Lupinus albus*) and common bean (*Phaseolus vulgaris*) under Pi sufficiency (Liu et al., 2005, 2010). More definitive evidence for the role of sugar in the response to Pi starvation came from the finding that the Arabidopsis *hsp1* (*hypersensitive to phosphate starvation1*)mutant (which overexpresses the sucrose transporter gene *SUC2*) is hypersensitive in almost all aspects of plant responses to Pi starvation and that the hexokinase signaling mutant *gin2* has altered expression of PSI genes (Karthikeyan et al., 2007; Lei et al., 2011a). However, whether light acts as an informational signal to regulate Pi signaling and PSRs remains unclear.

Numerous studies also support an important role for ethylene in regulating plant responses to Pi starvation. The expression of several *ACS* genes (*ACS2*, *ACS4*, and *ACS6*) and *ACO*, which encode enzymes for the conversion of AdoMet to ACC (1-aminocyclopropane-1-carboxylate) and ACC to ethylene (the two last steps in ethylene biosynthesis), is enhanced in Pi-starved Arabidopsis plants (Morcuende et al., 2007; Thibaud et al., 2010; Lei et al., 2011b). In addition, Pi deficiency also enhances plant sensitivity to ethylene, as reflected by changes in RSA and the induction of PSI gene expression (He et al., 1992; Basu et al., 2007; Lei et al., 2011b). Furthermore, the application of ethylene or ACC (the immediate precursor of ethylene) induces RSA changes that mimic the plant root responses triggered by Pi starvation. Similarly, Arabidopsis mutants that overproduce ethylene (*eto1* and *hps3*) or with a loss of function of the *ctr1* allele (*hsp2*) or bearing a mutation in the ethylene receptor gene *ERS1* (*hsp5*) also display a Pi deficiency-triggered root phenotype (reduced primary root elongation and increased production of root hairs) (K.L. Wang et al., 2004; Lei et al., 2011b; L. Wang et al., 2012; Song et al., 2016). These results provide compelling evidence for the role of ethylene in regulating Pi signaling and PSRs. However, the underlying molecular mechanisms remain poorly understood.

In this study, we show that the expression of *PHR1* is activated by light, which requires both the photoreceptors phytochrome A (phyA) and phytochrome B (phyB) for full activation. Light activation of *PHR1* expression is also dependent on FAR-RED ELONGATED HYPOCOTYL3 (FHY3) and FAR-RED-IMPAIRED RESPONSE1 (FAR1), a pair of positive regulators of phytochrome signaling. On the contrary, ELONGATED HYPOCOTYL5 (HY5), a bZIP transcription factor that acts downstream of all photoreceptors promoting photomorphogenesis, negatively regulates *PHR1* expression and alters PSRs in an opposite manner. Moreover, ETHYLENE-INSENSITIVE3 (EIN3), a transcription factor that acts as a key molecule in ethylene signaling, also directly binds to the *PHR1* promoter and regulates its expression. We provide molecular and genetic evidence that FHY3, FAR1, HY5, and EIN3 form a protein complex(es) to coordinately regulate *PHR1* expression and PSRs through signaling convergence at the *PHR1* promoter. We discuss the implications of our findings in the context of manipulating PSRs in crops for better adaptation to soils with limited Pi availability.

RESULTS

PHR1 Expression Is Induced by Light

To examine the possible effects of light on the transcriptional regulation of *PHR1* expression, we first examined the expression levels of *PHR1* in Arabidopsis seedlings grown under either constant light or dark conditions using qRT-PCR analysis. *PHR1* expression was considerably higher in light-grown seedlings than in dark-grown seedlings, with or without Pi supplementation in the medium (Figure 1A). To confirm this observation, we generated *ProPHR1:GUS* transgenic Arabidopsis lines to monitor light-dependent *PHR1* expression in planta. As shown in Figure 1B, GUS staining was much stronger in light-grown seedlings compared with dark-grown seedlings. Moreover, by measuring *PHR1* expression under different fluence rates, we found that *PHR1* transcript levels were positively correlated with the intensity of light (Figure 1C). Furthermore, the expression levels of eight PSI genes that function downstream of *PHR1* (*RNS1*, *IPS1*, *SPX1*, *SQD1* [*SULFOQUINOVOSYLDIACYLGLYCEROL1*], anthocyanidin 5-*O*-glucosyltransferase gene *PRE8*, *PMH1*, *ACP5* [*ACID PHOSPHATASE TYPE5*], and *PHF1* [*PHOSPHATE TRANSPORTER TRAFFIC FACILITATOR1*]) (Rubio et al., 2001; Cardona-López et al., 2015) were significantly lower in dark-grown seedlings compared with light-grown seedlings (Supplemental Figure 1A). These observations indicate that light activates *PHR1* expression.

To examine whether red/far-red light photoreceptors are involved in the light-induced activation of *PHR1*, we compared the expression levels of *PHR1* in the wild type, *phyA* and *phyB* single mutants, *phyA phyB* double mutant, and *phyABDE* quadruple mutant grown under white light conditions. In the presence of Pi, *PHR1* expression was notably reduced in the *phyA* and *phyB* single mutants and more dramatically reduced in the *phyA phyB* double and *phyABDE* quadruple mutants compared with the wild type. Intriguingly, *PHR1* expression was much more severely reduced in the *phyA phyB* double and *phyABDE* quadruple mutants in the absence of Pi (Figure 1D). These observations suggest that phytochrome-mediated light induction of *PHR1* expression might be Pi-dependent. Consistent with a positive role for phyA and phyB in Pi signaling, we found that Pi starvation-induced anthocyanin accumulation, total Pi accumulation, and Pi starvation-inhibited primary root elongation were attenuated in the *phyA* and

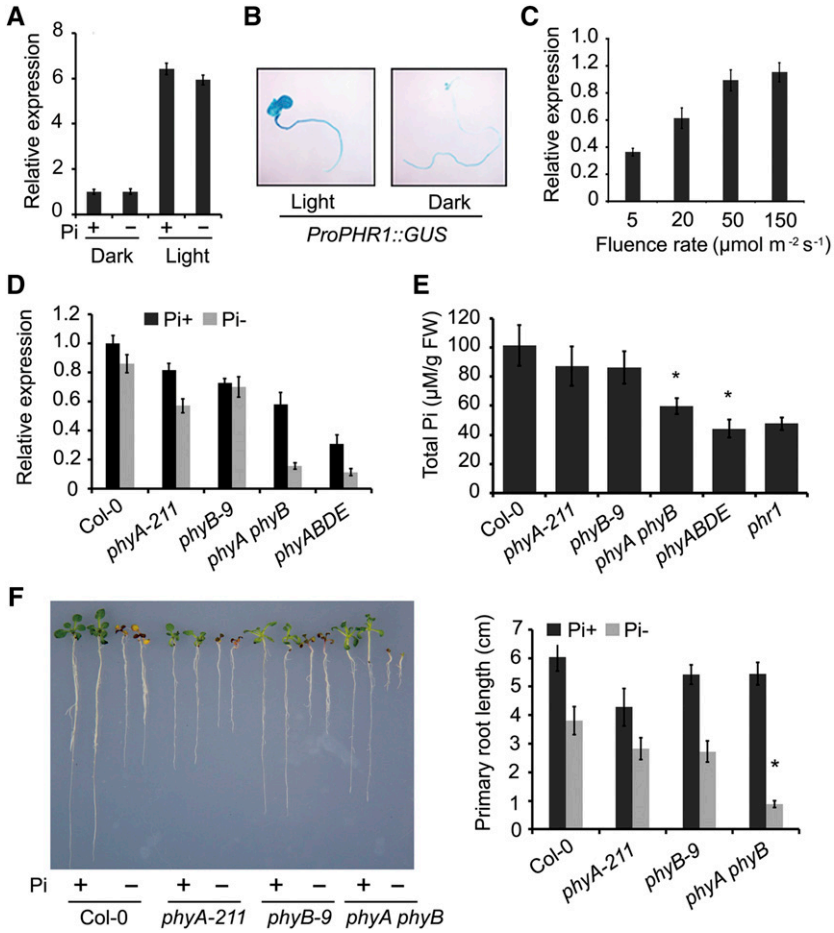

Figure 1. *PHR1* Expression Is Induced by Light.

(A) qRT-PCR analysis of *PHR1* expression in light- and dark-grown wild-type seedlings (Col-0). Six-day-old seedlings grown on MS +Pi and MS −Pi medium were collected for RNA extraction.

(B) Histochemical staining of *ProPHR1:GUS* seedlings grown under continuous light and dark conditions.

(C) qRT-PCR analysis of *PHR1* expression in 6-d-old wild-type (Col-0) seedlings grown under continuous white light of different intensities (fluence rates).

(D) qRT-PCR analysis of *PHR1* expression in light-grown wild-type (Col-0) and phytochrome mutant (*phyA-211*, *phyB-9*, *phyA phyB*, and *phyABDE*) plants. Samples were collected from 6-d-old seedlings grown on MS +Pi and MS −Pi medium.

(E) Histogram showing Pi content in wild-type (Col-0), *phyA-211*, *phyB-9*, *phyA phyB*, and *phr1* plants. Ten-day-old seedlings grown on Pi-supplemented medium (1 mM) were collected for Pi content measurement. Error bars indicate SD ($n = 20$). Asterisks indicate a significant differences from wild-type (Col-0) plants ($P < 0.05$, Student's *t* test). FW, fresh weight.

(F) Comparison of the primary root lengths of wild-type (Col-0), *phyA-211*, *phyB-9*, and *phyA phyB* plants grown under continuous white light on MS +Pi and MS −Pi medium. The asterisk indicates a significant difference from wild-type (Col-0) plants ($P < 0.05$, Student's *t* test).

phyB mutants, and severely inhibited in the *phyA phyB* mutant, compared with the wild type (Figures 1E and 1F; Supplemental Figures 1B and 2).

FHY3 and FAR1 Positively Regulate, While HY5 Negatively Regulates, *PHR1* Expression

We hypothesized that the activation of *PHR1* by light is mediated by pivotal light signaling factors. Earlier studies have shown that Arabidopsis FHY3 and its homolog FAR1 represent two transposase-derived transcription factors essential for phytochrome signaling (Hudson et al., 1999; Wang and Deng, 2002; Siddiqui et al., 2016). HY5 is a bZIP transcription factor that acts downstream of various photoreceptors to promote photomorphogenesis (Osterlund et al., 2000). To investigate whether FHY3, FAR1, and HY5 are involved in regulating *PHR1* expression, we compared *PHR1* expression levels in the wild type (No-0 and Col-0), *fhy3-4*, the *fhy3-4 far1-2* double mutant (No-0 ecotype), and the *hy5-215* mutant (Col-0 ecotype) grown under light and dark conditions. qRT-PCR showed that the light-induced increase in *PHR1* and PSI gene expression was significantly reduced in the *fhy3-4* and *fhy3-4 far1-2* mutants but dramatically elevated in the

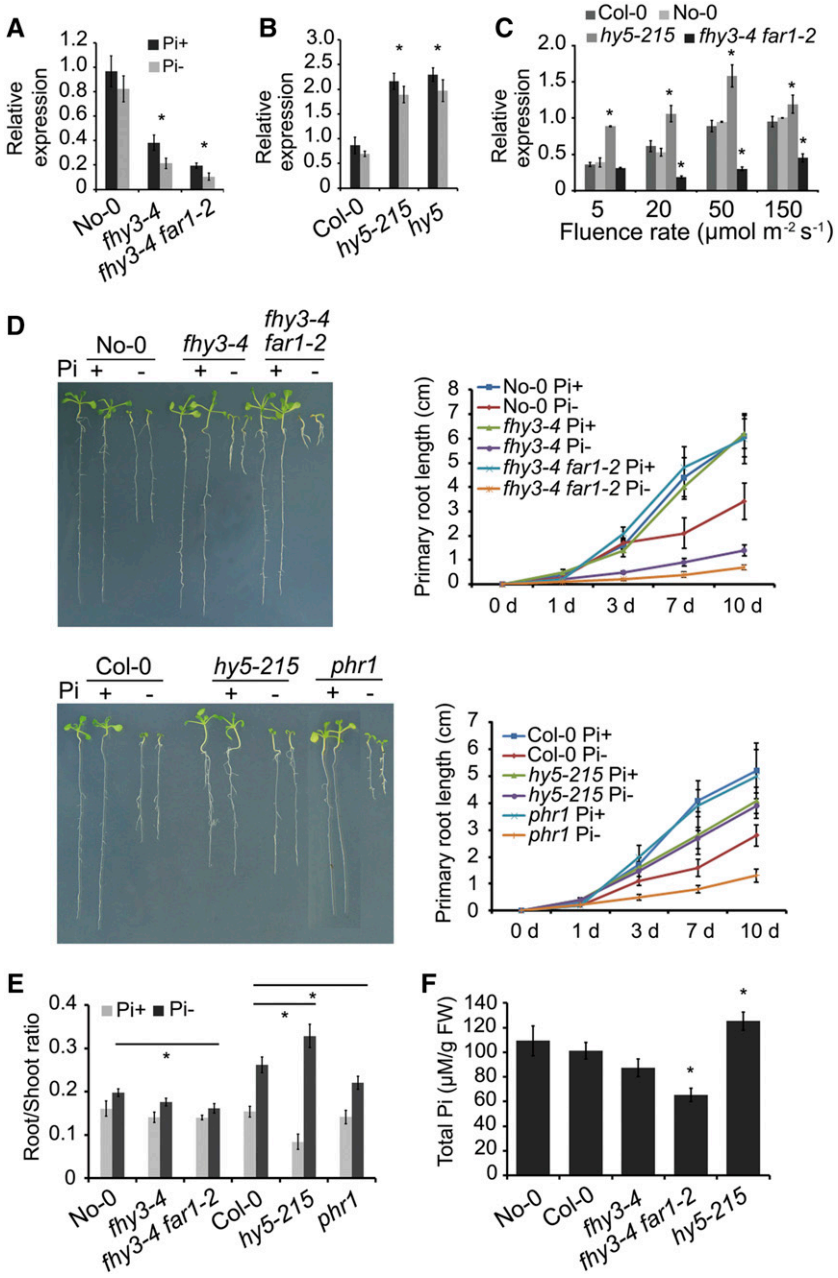

Figure 2. FHY3 and FAR1 Positively Regulate, While HY5 Negatively Regulates, *PHR1* Expression and Pi Starvation Responses.

(A) and **(B)** qRT-PCR analysis of *PHR1* expression in wild-type (No-0 and Col-0), *fhy3-4*, *fhy3-4 far1-2*, *hy5-215*, and *hy5* seedlings. Six-day-old seedlings grown under continuous white light on MS +Pi and MS −Pi medium were collected for RNA extraction. Asterisks indicate significant differences from wild-type (Col-0) plants ($P < 0.05$, Student's *t* test). Values are means ± SD; $n = 3$.

(C) qRT-PCR analysis of *PHR1* expression in wild-type (No-0 and Col-0), *fhy3-4*, *fhy3-4 far1-2*, and *hy5-215* seedlings (all 6 d old) grown under different fluence rates of white light. Asterisks indicate significant differences from wild-type (Col-0) plants ($P < 0.05$, Student's *t* test).

(D) Comparison of the primary root lengths of wild-type (No-0 and Col-0) with *fhy3-4*, *fhy3-4 far1-2*, *hy5-215*, and *phr1* seedlings grown under continuous white light on MS +Pi and MS −Pi medium. At least 20 seedlings for each genotype were measured.

(E) Histogram of root-to-shoot fresh weight ratios of wild-type (No-0 and Col-0), *fhy3-4*, *fhy3-4 far1-2*, *hy5-215*, and *phr1* mutant seedlings. Five-day-old seedlings grown on MS +Pi medium were transferred to MS +Pi or MS −Pi medium for 7 d before measurement. Asterisks indicate significant differences from wild-type (Col-0) plants ($P < 0.05$, Student's *t* test). Values are means ± SD; $n = 20$.

(F) Histogram showing Pi contents in wild-type (No-0 and Col-0), *fhy3-4*, *fhy3-4 far1-2*, and *hy5-215* mutant seedlings. Ten-day-old seedlings grown on MS +Pi medium (1 mM) were collected for measurement. Error bars indicate SD ($n = 20$). Asterisks indicate significant differences from wild-type (Col-0) plants ($P < 0.05$, Student's *t* test). FW, fresh weight.

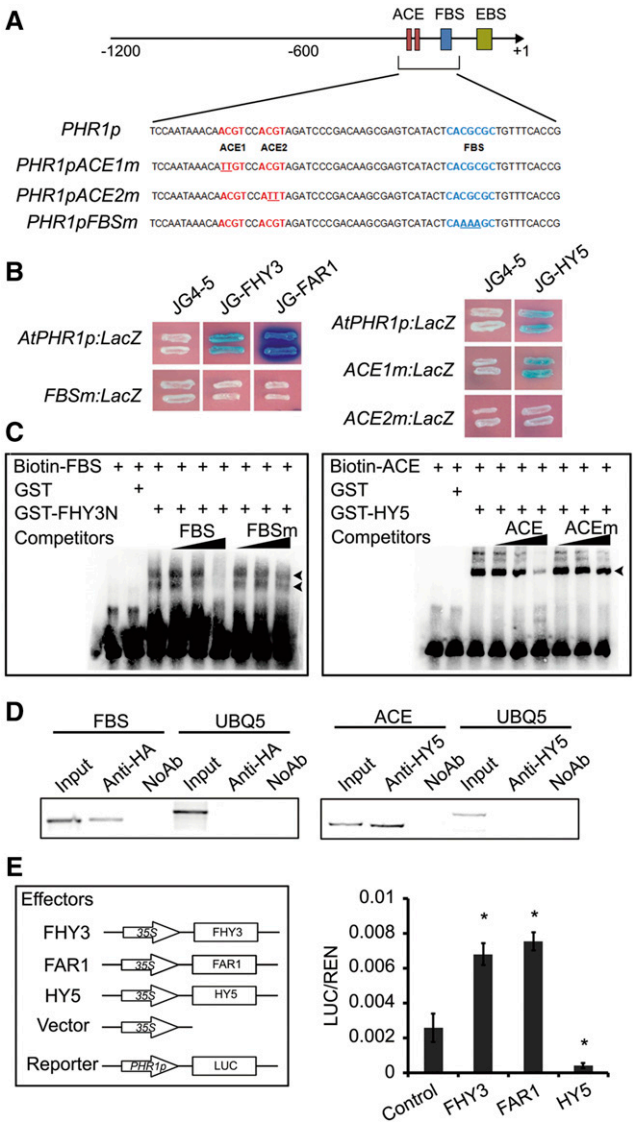

Figure 3. FHY3, FAR1, and HY5 Bind Directly to the *PHR1* Promoter.

(A) Diagram showing the *PHR1* promoter fragments and the putative binding sites of FHY3, FAR1, and HY5. The mutations within each element are shown below in red and blue.

(B) Yeast one-hybrid assay showing that FHY3 and FAR1 bind to the *PHR1* promoter through the FBS and that HY5 binds to the *PHR1* promoter through the ACE2 site. Empty vector expressing the AD alone was used as the negative control.

(C) Competitive EMSA showing that GST-FHY3N (left) and GST-HY5 (right) specifically bind to the *PHR1p-FBS* and *PHR1p-ACE* probes, respectively. The arrowheads indicate N-terminal GST-FHY3 and full-length GST-HY5 proteins. Five-, 10-, and 50-fold molar excesses of unlabeled probes were used in the competition assay.

(D) ChIP PCR showing binding of FHY3 and HY5 to the *PHR1* promoter in vivo. Seven-day-old *Pro35S:FLAG-FHY3-HA* (left) and wild-type (right) plants were harvested for ChIP. Primers used for ChIP PCR were specific to the promoter regions containing the FBS or ACE2 site. NoAb (no-antibody) precipitates and UBQ5 served as negative controls. The qPCR results were normalized against the input samples. Values are means ± SD; $n = 3$.

hy5-215 mutant (Figures 2A and 2B; Supplemental Figures 3A and 3B). Similarly, light intensity-associated increase in *PHR1* expression was also attenuated in the *fhy3-4 far1-2* mutant but enhanced in the *hy5-215* mutant (Figure 2C). In addition, when grown on Pi-deficient medium, the *fhy3-4* and *fhy3-4 far1-2* mutants displayed a severe inhibition of primary root elongation, similar to that of the *phr1* mutant (Figure 2D). In response to Pi deficiency, the increased root-to-shoot ratio was also significantly reduced in the *fhy3-4* and *fhy3-4 far1-2* mutants, but significantly increased in the *hy5-215* mutant, compared with the wild type (Figure 2E). Furthermore, we found that Pi contents and anthocyanin accumulation were reduced in the *fhy3-4* mutant and significantly reduced in the *fhy3-4 far1-2* mutant but increased in the *hy5-215* mutant compared with the wild type (Figure 2F; Supplemental Figure 3C). These observations suggest that FHY3 and FAR1 positively regulate, while HY5 negatively regulates, *PHR1* expression and PSRs. This notion was further supported by the observation that Pi limitation-mediated PSI gene induction and primary root inhibition were partially rescued in the *fhy3-4 far1-2 Pro35S:PHR1* transgenic lines and repressed in the *hy5-215 phr1* double mutant (Supplemental Figure 4).

FHY3, FAR1, and HY5 Directly Bind to the *PHR1* Promoter

We next examined whether FHY3, FAR1, and HY5 regulate *PHR1* expression by directly binding to its promoter. Bioinformatic analyses of *cis*-elements in the *PHR1* promoter identified two HY5 binding sites (ACGT-containing elements [ACEs]) (Osterlund et al., 2000) and one FHY3/FAR1 binding site (FBS; CACGCGC) (Lin et al., 2007) (Figure 3A). A yeast one-hybrid assay and electrophoretic mobility shift assay (EMSA) showed that FHY3, FAR1, and HY5 were able to bind specifically to the FBS and ACE2 elements, respectively (Figures 3B and 3C). The binding of FHY3 and HY5 to the *PHR1* promoter was further verified by a chromatin immunoprecipitation (ChIP) assay (Figure 3D). All of these results suggest that FHY3, FAR1, and HY5 regulate *PHR1* expression through direct binding to the *PHR1* promoter.

To further investigate the regulatory role of FHY3, FAR1, and HY5 in *PHR1* expression, we performed a transient expression assay using *Nicotiana benthamiana* leaves. We found that FHY3 and FAR1 activated, while HY5 repressed, *PHR1* expression (Figure 3E). We also characterized *PHR1* expression in *ProFHY3:FHY3-GR* (glucocorticoid receptor) and *ProHY5:HY5-GR* transgenic lines in response to dexamethasone (DEX) treatment, which releases the cytoplasmically retained FHY3-GR and HY5-GR fusion proteins into the nucleus to activate downstream gene expression (Lin et al., 2007). As expected, our qRT-PCR data showed that *PHR1* expression was significantly elevated in the *ProFHY3:FHY3-GR* transgenic plants, but reduced in the *ProHY5:HY5-GR* transgenic seedlings, in response to DEX application (Supplemental Figure 5).

(E) Transient expression assay showing that FHY3 and FAR1 activate *PHR1* expression while HY5 represses *PHR1* expression. *N. benthamiana* leaves were infiltrated with different combinations of effectors and reporter. Firefly luciferase activity was normalized to *Renilla* luciferase activity as an internal control. Asterisks indicate significant differences from the control ($P < 0.05$, Student's *t* test). Values are means ± SD; $n = 3$.

EIN3 and EIL1 Are Required for Ethylene-Induced Promotion of *PHR1* Expression

To investigate whether ethylene plays a role in regulating *PHR1* expression, we examined the effect of ACC on *PHR1* and PSI gene expression. As previously reported (Wang et al., 2012), light-grown Arabidopsis seedlings treated with ACC phenocopied those grown under −Pi conditions, while treatment with Ag^+ (an inhibitor of ethylene action) rescued the retarded primary root growth phenotype (Supplemental Figure 6). qRT-PCR analysis showed that the transcript levels of *PHR1* and the PSI genes examined were enhanced by ACC treatment (Figures 4A and 4B), suggesting that ethylene positively regulates *PHR1* and PSI gene expression.

Given that EIN3 and its closest homolog ETHYLENE-INSENSITIVE3-Like1 (EIL1) are two master transcription factors essential for ethylene signaling (Guo and Ecker, 2003), we next examined their effect on *PHR1* and PSI gene expression. qRT-PCR analysis revealed that the transcript levels of *PHR1* were reduced in the *ein3-1 eil1-1* double mutant with or without ACC treatment (Figure 4A). Similarly, the induction of PSI genes was also attenuated in the *ein3-1 eil1-1* mutant in response to Pi starvation or ACC treatment compared with the wild type (Figure 4B; Supplemental Figure 7). These results suggest that EIN3 and EIL1 play an essential role in mediating ethylene-induced promotion of *PHR1* expression and the response to Pi starvation. Consistent with this notion, the Pi starvation-induced inhibited primary root elongation, reduced root-to-shoot ratio, and total Pi accumulation were all impaired in the *ein3-1* mutant compared with the wild type (Figures 4C to 4E; Supplemental Figure 4).

Sequence analysis identified a palindromic repeat sequence similar to the EIN3 binding site (named EBS) (Solano et al., 1998) in region III of the *PHR1* promoter. A yeast one-hybrid assay showed that EIN3 directly bound to the *PHR1* promoter and specifically recognized the EBS sequence (Figures 4F and 4G). Mutagenesis of EBS (*EBSm*) confirmed that the nucleotides around *EBS* were crucial for this binding (Figure 4G). This binding was further verified by in vitro EMSA and in vivo ChIP PCR assays using transgenic plants expressing EIN3-FLAG fusion protein under the control of an estradiol-inducible promoter (An et al., 2010) (Figures 4H and 4I). Moreover, *PHR1* expression also increased in a time-dependent manner in the estradiol-inducible EIN3-FLAG transgenic plants after β-estradiol treatment (Supplemental Figure 8). Transient expression analysis in *N. benthamiana* also revealed that co-expression of *EIN3* dramatically increased the expression of the *ProPHR1:LUC* reporter gene (Figure 4J). Furthermore, Pi starvation-mediated increased PSI gene expression and primary root inhibition were largely restored in the *ein3-1 Pro35S:PHR1* transgenic lines compared with wild-type plants (Supplemental Figure 4). Together, these results support the notion that EIN3 directly activates *PHR1* expression to mediate the ethylene-induced regulation of PSRs.

FHY3 Directly Interacts with EIN3

Given the close proximity between the binding sites of FHY3 (and FAR1), HY5, and EIN3 (and EIL1) proteins on the *PHR1* promoter, we next examined whether these transcription factors might interact with one another. A yeast two-hybrid assay showed that both FHY3 and FAR1, but not HY5, interacted with EIN3 and EIL1 (Figure 5A). To define the domains responsible for their interactions, we used various deletion constructs of FHY3 and EIN3 fused with the LexA binding protein and the activation domain (AD), respectively. The results showed that although none of the three individual FHY3 domains (N-terminal C2H2 zinc finger domain, central putative core transposase domain, and C-terminal SWIM zinc finger domain; Lin et al., 2007) interacted with EIN3 in yeast, the central transposase domain and C-terminal SWIM domain together interacted with EIN3 (Figure 5B). We also mapped the domain of EIN3 responsible for its interaction with FHY3. As shown in Figure 5B, the central part ($EIN3^{141-352}$) containing the DNA binding domain (Zhu et al., 2011) interacted with FHY3, whereas no detectable interaction was observed between FHY3 with the N-terminal part ($EIN3^{1-140}$) or the C-terminal part ($EIN3^{352-629}$) of EIN3. The FHY3-EIN3 interaction was also confirmed in a transient bimolecular fluorescence complementation (BiFC) assay using *N. benthamiana* leaf epidermal cells and a coimmunoprecipitation assay with transgenic plants coexpressing FHY3-HA and EIN3-FLAG (Figures 5C and 5D). Together, these results suggest that FHY3, FAR1, and EIN3 form a transcriptional regulatory complex(es) on the *PHR1* promoter in vivo to coordinately regulate its expression in response to light and ethylene.

FHY3 and EIN3 Coordinately Regulate *PHR1* Expression and PSRs

To investigate the combined effect of light and ethylene treatment on *PHR1* expression, we compared the expression levels of *PHR1* in light- and dark-grown seedlings treated with or without ACC. otably, the elevated expression of *PHR1* and Pi starvation-induced increased PSI gene expression in light-grown plants in response to ACC treatment were almost completely diminished in dark-grown plants and significantly attenuated in light-grown *fhy3-4 far1-2* mutant plants (Figures 6A and 6B; Supplemental Figure 9). These results suggest that the regulation of *PHR1* expression and PSRs by ethylene requires active light signaling as well as FHY3 and FAR1 proteins. Consistent with this observation, coexpression of FHY3 and EIN3 proteins activated the expression of the *ProPHR1:LUC* reporter gene to a higher level compared with FHY3 or EIN3 alone in *N. benthamiana* leaves (Figure 6C). Additionally, a luciferase complementation imaging (LCI) assay of *N. benthamiana* revealed that the interaction between FHY3 and EIN3 mainly occurred in the light (Supplemental Figure 10). For further genetic validation of the proposed interaction between FHY3 and EIN3, we generated the *fhy3-4 ein3-1* double mutant. *PHR1* expression was further reduced in the *fhy3-4 ein3-1* double mutant compared with the *fhy3-4* and *ein3-1* single mutants (Figure 6D). Inhibition of primary root growth on Pi starvation medium was also more pronounced in the *fhy3-4 ein3-1* double mutant compared with the *fhy3-4* and *ein3-1* single mutants (Figure 6E). Furthermore, total Pi content was more severely reduced in the *fhy3-4 ein3-1* double mutant compared with the two single parental mutants (Figure 6F). The combined data suggest that FHY3 and EIN3 coordinately regulate *PHR1* expression and PSRs.

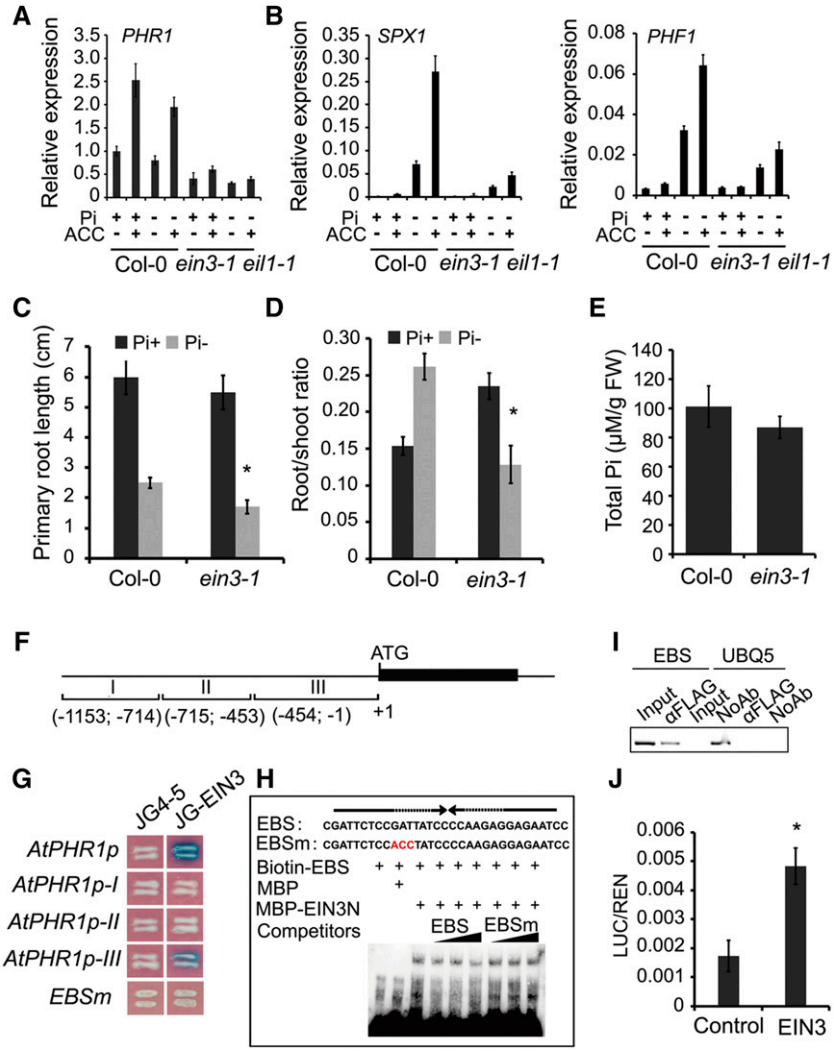

Figure 4. EIN3 Is Required for Ethylene-Induced *PHR1* Expression and Pi Starvation Responses.

(A) and **(B)** qRT-PCR analysis of the expression of *PHR1* and PSI genes (*SPX1* and *PHF1*) in wild-type (Col-0) and *ein3-1 eil1-1* mutant plants grown under continuous white light conditions. For ACC treatment, 5-d-old seedlings grown on MS +Pi or MS −Pi medium were transferred to MS +Pi or MS −Pi medium supplemented with 10 μM ACC for 2 d before the assay.

(C) Comparison of the primary root lengths of 10-d-old wild-type (Col-0) and *ein3-1* seedlings grown on MS +Pi or MS −Pi medium. At least 20 seedlings for each genotype were measured. The asterisk indicates a significant difference from wild-type (Col-0) plants ($P < 0.05$, Student's *t* test).

(D) Histogram of root-to-shoot fresh weight ratios of the wild type (Col-0) and the *ein3-1* mutant. Five-day-old seedlings grown on MS +Pi medium were transferred to MS +Pi or MS −Pi medium for 7 d before the measurement. The asterisk indicates a significant difference from wild-type (Col-0) plants ($P < 0.05$, Student's *t* test). Values are means ± SD; $n = 20$.

(E) Histogram showing total Pi content in 10-d-old wild-type (Col-0) and *ein3-1* seedlings grown on MS +Pi medium (1 mM). FW, fresh weight.

(F) Diagram of the three *PHR1* promoter regions used for the yeast one-hybrid assay.

(G) Yeast one-hybrid assay showing that EIN3 binds to the *PHR1* promoter through the EBS within promoter region III. The *LacZ* reporter gene was driven by the full-length *AtPHR1* promoter or by *AtPHR1-I*, *AtPHR1-II*, *AtPHR1-III*, or *EBSm* fragments. Empty vector expressing the AD alone was used as the negative control.

(H) EMSA showing that EIN3 binds to the EBS element in vitro. Wild-type EBS sequence is shown with the palindromic repeats indicated by arrows. The mutated nucleotides in EBSm are shown in red. Five-, 10-, or 50-fold molar excesses of unlabeled probes were used in the competition reactions.

(I) ChIP assay showing that EIN3 binds to the *PHR1* promoter in vivo. Seven-day-old EIN3-FLAG seedlings pretreated with 10 μM β-estradiol were harvested for ChIP. Primers used for ChIP PCR were specific to the promoter region containing the EBS element. NoAb (no-antibody) precipitates and UBQ5 served as the negative controls. The qPCR results were normalized against the input samples. Values are means ± SD; $n = 3$.

(J) Transient expression assay showing that EIN3 promotes *ProPHR1:LUC* expression. Firefly luciferase activity was normalized to *Renilla* luciferase activity as an internal control. The asterisk indicates a significant difference from the control ($P < 0.05$, Student's *t* test). Values are means ± SD; $n = 3$.

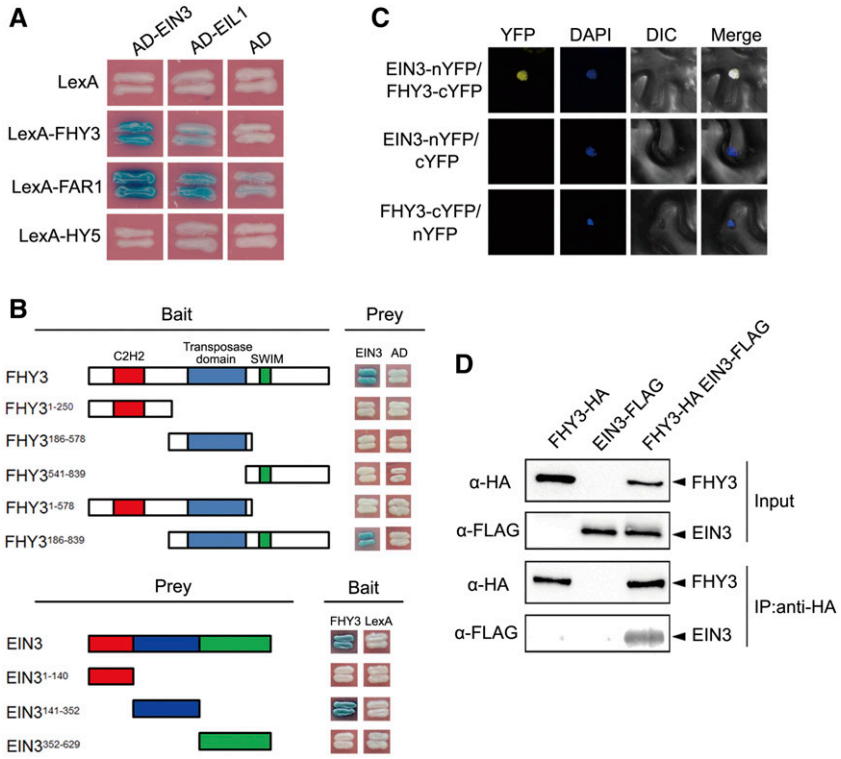

Figure 5. FHY3 Interacts with EIN3 in Vitro and in Vivo.

(A) Yeast two-hybrid assay showing that FHY3 and FAR1 interact with EIN3 and EIL1.
(B) Mapping of the domains involved in the FHY3-EIN3 interaction using yeast two-hybrid assays. Different domains of FHY3 were fused with the LexA domain in pEG202, whereas different domains of EIN3 were fused with the AD in pB42AD. LexA and AD served as the negative controls.
(C) BiFC assay showing interaction between FHY3 and EIN3 in *N. benthamiana* leaf epidermal cells. EIN3 was fused to the N-terminal fragment of YFP (nYFP); FHY3 was fused to the C-terminal fragment of YFP (cYFP). Nuclei were counterstained with 4′,6-diamidino-2-phenylindole (DAPI). DIC, differential interference contrast.
(D) Coimmunoprecipitation assay showing that FHY3 associates with EIN3 in planta. Protein extracts from 6-d-old seedlings expressing FHY3-HA and EIN3-FLAG were pretreated with 10 μM β-estradiol for 10 h. Plant extracts were then immunoprecipitated using anti-HA antibody, separated on a 10% SDS-PAGE gel, and blotted with anti-HA (1:4000) or anti-FLAG (1:4000) antibody.

HY5 Represses FHY3/EIN3-Induced Activation of *PHR1* Expression

We next investigated whether HY5 affects the transcriptional activity of FHY3 and EIN3 on *PHR1*. As shown in Figure 7A, coexpression of HY5 significantly repressed FHY3- and EIN3-induced activation of the *ProPHR1:LUC* reporter gene in *N. benthamiana* leaf epidermal cells. A previous study showed that the interaction of FHY3 and HY5 is mediated through their DNA binding domains (Li et al., 2010). Thus, we investigated whether HY5 affects the binding of FHY3 to the *PHR1* promoter via an EMSA. As shown in Figure 7B, the occupancy of FHY3 on the *PHR1* promoter gradually decreased as increasing amounts of HY5 protein were added into the assay, suggesting that HY5 competes with FHY3 for binding to the *PHR1* promoter. In support of this notion, we compared the binding ability of FHY3 on the *PHR1* promoter in wild-type and *hy5-215* mutant plants. As expected, stronger FHY3 association with the *PHR1* promoter was observed in the *hy5-215* mutant (Figure 7C). Additionally, the *hy5-215* mutation partially rescued the primary root phenotype and restored the *PHR1* expression level in *fhy3-4 far1-2* under Pi-limited conditions (Figures 7D and 7E). Similarly, the *hy5-215* mutation partially rescued the inhibited primary root growth phenotype and *PHR1* expression in the *hy5-215 ein3-1* double mutant (Figures 7F and 7G). Taken together, these results prompted us to conclude that HY5 represses the activity of FHY3 and EIN3 on *PHR1* gene expression, most likely through protein-protein interactions.

The Stability of FHY3 and HY5 Is Modulated by Light and Ethylene

Since FHY3 and FAR1 are required for both light- and ethylene-mediated induction of *PHR1* expression, we next examined how light and ethylene might regulate FHY3 protein accumulation. Immunoblot analysis showed that FHY3 protein levels increased dramatically when dark-grown *Pro35S:FLAG-FHY3-HA* transgenic seedlings were transferred to the light (Figure 8A). Interestingly, ACC treatment also promoted FHY3 protein accumulation in light-grown seedlings (Figure 8B). Confocal microscopy examination

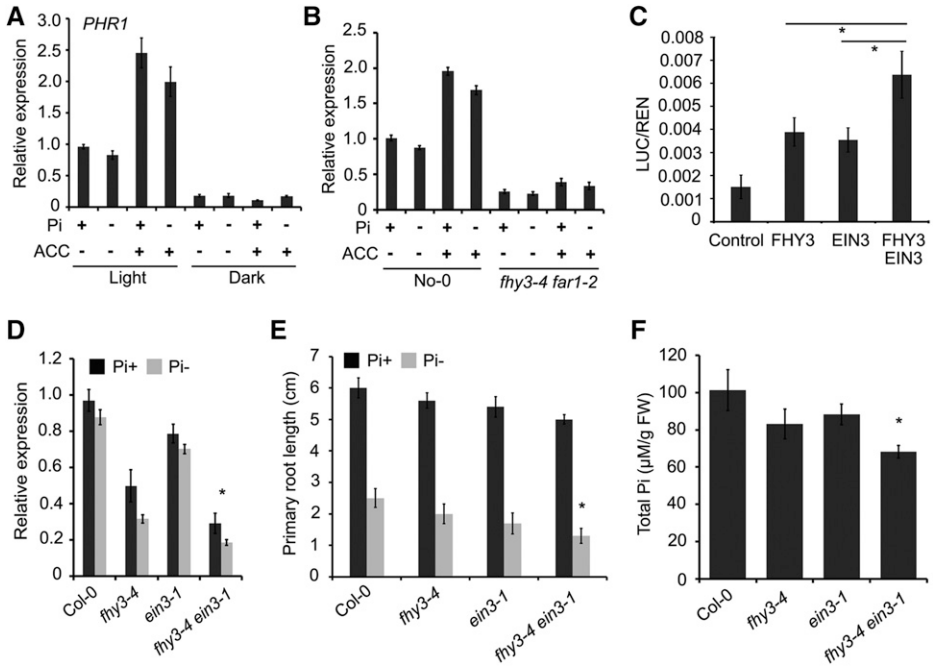

Figure 6. FHY3 and EIN3 Coordinately Promote *PHR1* Expression and Phosphate Starvation Responses.

(A) qPCR analysis of *PHR1* expression in light- and dark-grown wild-type (Col-0) plants. For ACC treatment, 5-d-old seedlings grown on MS +Pi medium were transferred to MS +Pi or MS −Pi medium supplemented with 10 μM ACC for 2 d before RNA extraction. Values are means ± SD; $n = 3$.

(B) qPCR analysis of *PHR1* expression in light-grown wild-type (No-0) and *fhy3-4 far1-2* seedlings. Five-day-old seedlings grown on MS +Pi medium were transferred to fresh MS medium supplemented with 10 μM ACC for 2 d before RNA extraction. Values are means ± SD; $n = 3$.

(C) Transient expression assay using *N. benthamiana* leaves. *N. benthamiana* leaves were infiltrated with *A. tumefaciens* transformed with the indicated reporter and effector constructs. Relative LUC activity normalized to REN activity is shown (LUC/REN). Values are means ± SD; $n = 3$. The pSPYNE-35S empty vector was used as the control. Asterisks indicate significant differences from the control ($P < 0.05$, Student's *t* test).

(D) qRT-PCR analysis of *PHR1* expression in wild-type (Col-0), *fhy3-4*, and *fhy3-4 ein3-1* mutant seedlings. Six-day-old seedlings grown under continuous white light on MS +Pi and MS −Pi medium were collected for RNA extraction. The asterisk indicates a significant difference from *fhy3-4* and *ein3-1* mutant plants ($P < 0.05$, Student's *t* test).

(E) Comparison of the primary root lengths of wild-type (Col-0), *fhy3-4*, *ein3-1*, and *fhy3-4 ein3-1* seedlings grown under continuous white light on MS +Pi and MS −Pi medium and collected for RNA extraction. Values are means ± SD (at least 20 seedlings for each genotype were measured). The asterisk indicates a significant difference from wild-type (Col-0) plants ($P < 0.05$, Student's *t* test).

(F) Histogram showing Pi contents in 10-d-old wild-type (Col-0), *fhy3-4*, *ein3-1*, and *fhy3-4 ein3-1* seedlings grown on MS +Pi medium (1 mM). Values are means ± SD; $n = 20$. The asterisk indicates a significant difference from *fhy3-4* and *ein3-1* mutant plants ($P < 0.05$, Student's *t* test). FW, fresh weight.

revealed that light or ACC treatment substantially enhanced the nuclear abundance of FHY3-YFP in *ProFHY3:FHY3-YFP* transgenic plants (Figures 8C to 8F). EIN3 is stabilized by ethylene and Pi starvation (Guo and Ecker, 2003; Song et al., 2016). HY5 is stabilized by light but destabilized by ethylene treatment (Osterlund et al., 2000; Yu et al., 2013). Consistent with these findings, we found that ACC treatment blocked HY5 protein accumulation in light-grown seedlings (Figures 8G to 8I).

DISCUSSION

Plants have evolved elaborate mechanisms to integrate various environmental signals and internal developmental regulators to cope with Pi deficiency, which commonly occurs in nature. In this study, we present evidence showing that light and ethylene coordinately regulate *PHR1* expression and PSRs through signaling convergence at the *PHR1* promoter.

Active Light Signaling Is Required for the Induction of *PHR1* Expression and PSRs

Many studies have shown that sugars play an essential role in regulating PSRs, including increased expression of PSI genes and changes in RSA (Franco-Zorrilla et al., 2005; Liu et al., 2005; Karthikeyan et al., 2007; Lei et al., 2011a). Pi starvation can result in a reduction in photosynthesis efficiency and increased levels of sugars and starch in Pi-deprived leaves (Marschner, 1995; Chiou and Lin, 2011). It has been hypothesized that the movement of sugars or their metabolites is one of the major components required for the expression of PSI genes and increases in the root-to-shoot biomass ratio (López-Bucio et al., 2003; Karthikeyan et al., 2007). Several lines of evidence support such a notion. First, a stem-girdling experiment with white lupin showed that PSI gene expression in cluster roots is hampered by restricting the movement of solutes to roots (Liu et al., 2005). Second, the Arabidopsis *hsp1* mutant (which overexpresses

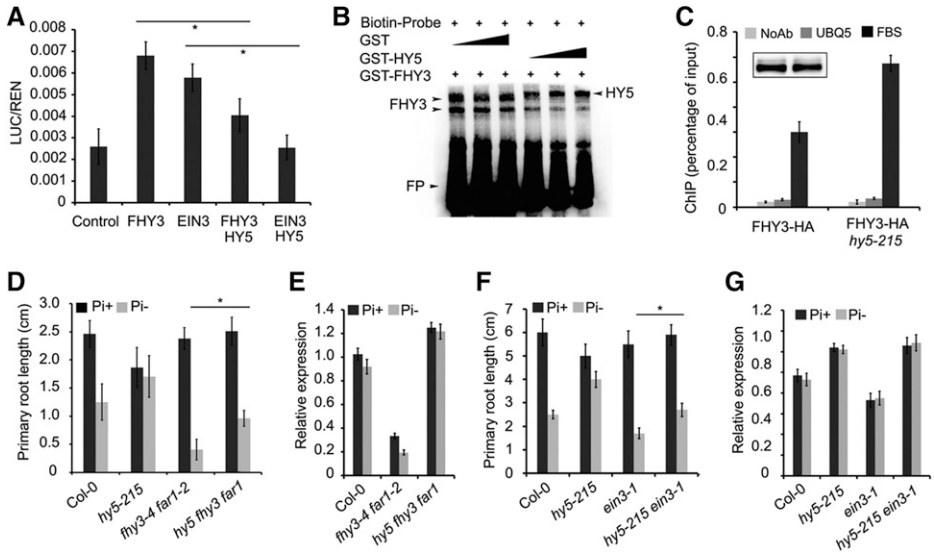

Figure 7. HY5 Suppresses FHY3 and EIN3 Activation of *PHR1* Expression.

(A) Transient expression assay using *N. benthamiana* leaves. The *N. benthamiana* leaves were infiltrated with *A. tumefaciens* transformed with the indicated reporter and effector constructs. The relative LUC activities normalized to the REN activity are shown (LUC/REN). Asterisks indicate significant differences from control ($P < 0.05$, Student's *t* test). Values are means ± SD; $n = 3$.

(B) EMSA showing that increasing amounts of GST-HY5 protein, but not GST, decrease the binding of GST-FHY3N to the wild-type *PHR1* promoter. Biotin-labeled probes containing FBS and ACE sites were added to the reaction.

(C) ChIP PCR results showing that FHY3 associates with the *PHR1* promoter in the *hy5-215* mutant background. Chromatin was extracted from the *Pro35S:FLAG-FHY3-HA* and *Pro35S:FLAG-FHY3-HA/hy5-215* transgenic seedlings and precipitated using anti-HA antibodies. Precipitated DNA was amplified with primers corresponding to the sequence of the FBS site in the *PHR1* promoter. The inset shows the amount of FHY3 protein in this assay. NoAb (no-antibody) precipitates and UBQ5 served as the negative controls. Values are means ± SD; $n = 3$.

(D) Comparison of the primary root lengths of 10-d-old wild-type (Col-0), *hy5-215*, *fhy3-4 far1-2*, and *fhy3 far1 hy5* seedlings grown on MS +Pi and MS −Pi medium. Six-day-old seedlings grown under continuous white light on MS +Pi and MS −Pi medium were collected for RNA extraction. The asterisk indicates a significant difference from wild-type (Col-0) plants ($P < 0.05$, Student's *t* test). Values are means ± SD (at least 20 seedlings for each genotype were measured).

(E) qRT-PCR analysis of *PHR1* expression in wild-type, *fhy3-4 far1-2*, and *hy5 fhy3 far1* mutant seedlings. Six-day-old seedlings grown under continuous white light on MS +Pi and MS −Pi medium were collected for RNA extraction. Values are means ± SD; $n = 3$.

(F) Comparison of the primary root lengths of wild-type (Col-0), *hy5-215*, *ein3-1*, and *hy5-215 ein3-1* seedlings grown on MS medium supplemented with or without Pi. The asterisk indicates a significant difference from wild-type (Col-0) plants ($P < 0.05$, Student's *t* test). Values are means ± SD (at least 20 seedlings for each genotype were measured).

(G) qRT-PCR analysis of *PHR1* expression in wild-type (Col-0), *hy5-215*, *ein3-1*, and *hy5-215 ein3-1* mutant seedlings. Six-day-old seedlings grown under continuous white light on MS +Pi and MS −Pi medium were collected for RNA extraction. Values are means ± SD; $n = 3$.

SUC2) is hypersensitive in almost all aspects of plant responses to Pi starvation (Lei et al., 2011a). Third, the hexokinase signaling mutant *gin2* also displays altered expression of PSI genes (Karthikeyan et al., 2007).

In this study, we show that the far-red and red photoreceptors phyA and phyB, respectively, and two light signaling transcription factors, FHY3 and FAR1, whose protein accumulation is promoted by light, are required for light-induced *PHR1* expression and PSRs. FHY3 and FAR1 were originally identified as crucial phyA signaling components, but they were recently shown to also act downstream of light-stable phytochromes, i.e., phyB, phyD, and phyE (Siddiqui et al., 2016). FHY3 and FAR1 have also been shown to play multifaceted roles in diverse developmental and physiological processes beyond light signaling (Wang and Wang, 2015). Our results are consistent with the earlier finding that PSI reporter activity decreases when light-grown seedlings on Pi-deficient medium were transferred to darkness (Karthikeyan et al., 2007). Unexpectedly, we found that HY5, another positive regulator of light signaling, represses *PHR1* and PSI gene expression and mediates PSRs in an opposite manner to that of FHY3 and FAR1. Consistent with the earlier finding that FHY3 and FAR1 directly interact with HY5 (Li et al., 2010; Li et al., 2011; Huang et al., 2012) and that HY5 represses the DNA binding activity of FHY3 (Li et al., 2010), we found that more FHY3 was immunoprecipitated in the *hy5* mutant background compared with the wild type (Figure 7C), suggesting that the binding of FHY3 to the *PHR1* promoter is negatively regulated by HY5 (there might be steric hindrance for FHY3 and HY5 binding to the *PHR1* promoter, as their binding sites are <30 bp apart; Figure 3A). On the other hand, we also showed that HY5 can directly bind to the *PHR1* promoter through the ACE (Figure 3B). Given the previous finding that HY5 has intrinsic transcriptional repression activity in vivo (Jing et al., 2013), we deduced that FHY3 and HY5 normally act antagonistically to regulate *PHR1* expression through their

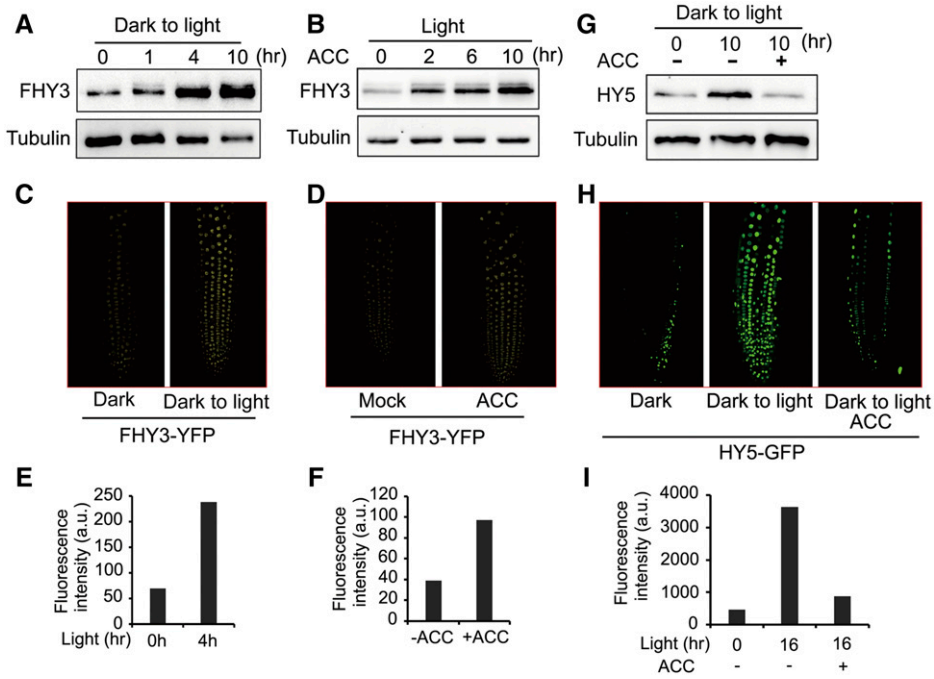

Figure 8. Light and Ethylene Promote FHY3 Accumulation, While Ethylene Destabilizes HY5.

(A) Immunoblot assay showing that FHY3 protein levels increase in dark-grown *Pro35S:FLAG-FHY3-HA* seedlings subsequently exposed to light treatment. Anti-FLAG (1:4000; MBL) was used to detect FHY3 protein. Tubulin was used as a loading control.

(B) Immunoblot assay showing that ACC treatment promotes FHY3 protein accumulation. Tubulin was used as a loading control. Anti-FLAG (1:4000; MBL) was used to detect FHY3 protein.

(C) and **(D)** Fluorescence microscopic analysis of FHY3-YFP protein levels. Five-day-old dark-grown *ProFHY3:FHY3-YFP/fhy3-4* seedlings **(C)** were exposed to light for 4 h. For ACC treatment **(D)**, yellow fluorescence was observed in 5-d-old *ProFHY3:FHY3-YFP/fhy3-4* seedlings after 10 h of treatment with 10 μM ACC.

(E) and **(F)** Quantification of fluorescence signals for **(C)** and **(D)**. The fluorescence intensity was quantified by measuring the fluorescence pixel intensity using ImageJ. a.u., arbitrary units.

(G) Immunoblot assay of HY5 protein accumulation in response to light and ACC treatments. Five-day-old dark-grown wild-type seedlings were transferred to MS medium or MS medium supplemented with 10 μM ACC, exposed to light, and collected at the indicated times. Anti-HY5 (1:1000) was used to detect HY5 protein. Tubulin was used as a loading control.

(H) Fluorescence microscopic analysis shows that light promotes HY5 protein accumulation, whereas treatment with 10 μM ACC blocks HY5 protein accumulation in *Pro35S:HY5-GFP* transgenic seedlings. Five-day-old dark-grown *Pro35S:HY5-GFP* transgenic seedlings were transferred to MS medium or MS medium supplemented with 10 μM ACC and then exposed to light for 16 h before examination (dark to light for 16 h).

(I) Quantification of GFP fluorescence signals for **(H)**.

protein-protein interaction, but in the absence of FHY3 and FAR1, HY5 is able to repress *PHR1* expression independently. The antagonistic action of FHY3/FAR1 with HY5 might define a feedback or fine-tuning mechanism for the homeostasis of Pi signaling. Together, our data and previous results suggest that light acts both as an energy source and as an informational signal for activating PSRs.

EIN3 and EIL1 Are Required for Ethylene-Mediated *PHR1* Expression and PSRs

These is ample evidence that ethylene plays an important role in regulating PSRs, particularly Pi deficiency-induced remodeling of RSA (reduced primary root elongation and increased production of lateral roots and root hairs) (Nagarajan and Smith, 2012; Song and Liu, 2015). This regulation may occur at several different levels. First, enhanced expression of ethylene biosynthetic genes (mainly *ACS* and *ACO*) in response to Pi starvation has been reported in several plant species (Kim et al., 2008; Li et al., 2009; Lei et al., 2011b). In addition, Pi deficiency can enhance plant sensitivity to ethylene, which likely involves changes in the expression of a group of ethylene-responsive transcription factors (He et al., 1992; Misson et al., 2005; Thibaud et al., 2010). Third, a recent study showed that the stability of EIN3 protein increases in response to Pi starvation (Song et al., 2016). In this study, we show that EIN3 and EIL1 are essential for ethylene- and Pi starvation-induced *PHR1* and PSI gene expression as well as PSRs (Figures 4A and 4B; Supplemental Figure 7). We further show that EIN3 could directly bind to the *PHR1* promoter and activate its expression. Our results suggest that EIN3 and EIL1 are critical regulators of ethylene-mediated Pi responses by directly regulating *PHR1* expression.

Coordinated Regulation of *PHR1* Expression by Light and Ethylene

Light and ethylene coordinately regulate many aspects of plant growth and development through signaling crosstalk (Yu et al., 2013; Zhong et al., 2014; Shi et al., 2016). In this study, we showed that light and ethylene appear to have an additive effect on induction of *PHR1* expression. Particularly interesting, we found that the induction of *PHR1* and PSI gene expression by ACC was almost abolished in dark-grown seedlings (Figures 4A and 4B), indicating an essential role of light in ethylene-mediated Pi signaling and PSRs. In addition, we found that ethylene-mediated Pi signaling and PSRs also depend on FHY3 and FAR1 (Figure 6B). We provided evidence that FHY3 directly interacts with EIN3 and that these proteins act additively to promote *PHR1* expression (Figures 5 and 6C). On the other hand, HY5 suppresses FHY3- and EIN3-induced activation of *PHR1* expression (Figure 7A). We showed that HY5 suppresses the transcriptional activation activity of FHY3, FAR1, and EIN3, most likely through competitive binding to their distinct *cis*-elements on the *PHR1* promoter. This result is consistent with the earlier finding that HY5 negatively regulates FHY3/FAR1-activated *FHY1*/*FHL* expression under far-red light (Li et al., 2010). Furthermore, we showed that both light and ethylene promote the accumulation of FHY3 protein, whereas light-induced promotion of HY5 protein accumulation is blocked by ACC treatment (Figure 8G). Based on these findings and the previous findings that both light and ethylene promote EIN3 protein accumulation (Guo and Ecker, 2003; Shi et al., 2016) but ethylene destabilizes HY5 (Yu et al., 2013), we propose a molecular model for the coordinated regulation of PSRs by light and ethylene through signaling convergence at the *PHR1* promoter. Light and ethylene act to promote *PHR1* expression and PSRs via promoting the accumulation of FHY3 and EIN3, two positive regulators of *PHR1* expression. In addition, ethylene abrogates the repressive effect of HY5 on *PHR1* expression by blocking HY5 protein accumulation (Figure 9).

Notably, examination of the reported genome-wide binding sites of FHY3, HY5, and EIN3 (Lee et al., 2007; Ouyang et al., 2011; Zhang et al., 2011; Chang et al., 2013) revealed high percentages of shared target genes among these three transcription factors (Supplemental Figure 11A and Supplemental Data Set 1). It has been shown that FHY3 and HY5 physically interact with each other and coregulate a large number of common target genes, and the physiological relevance of several interactions has been demonstrated (Li et al., 2010; Li et al., 2011; Ouyang et al., 2011; Huang et al., 2012). In silico examination also revealed that a large number of EIN3 targets are likely coregulated by HY5 (Supplemental Figure 11A), implying that these protein-protein interactions might represent a general mechanism for regulating downstream gene expression and physiological responses. Gene Ontology (GO) analysis of the putative common targets of FHY3, HY5, and EIN3 showed that genes involved in developmental processes and response to stimulus are highly enriched (Supplemental Figure 11B). However, more detailed molecular and biochemical studies are required to substantiate the coregulation of other target genes by these transcription factors in future studies.

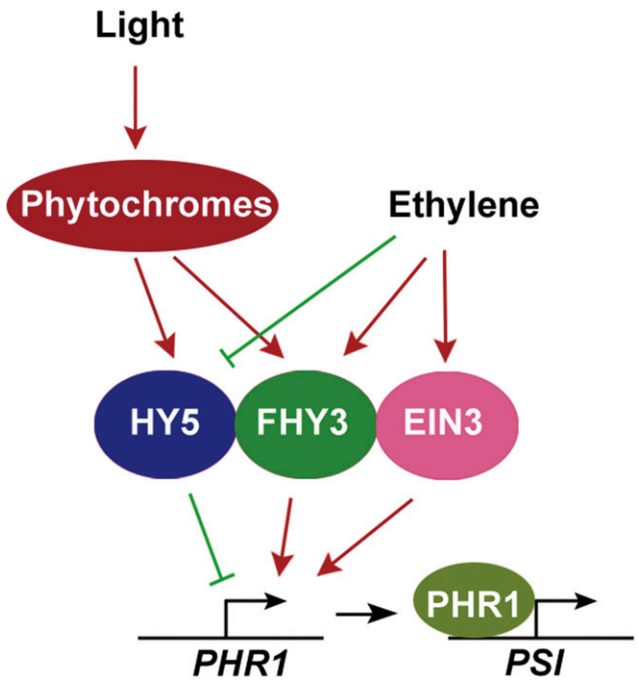

Figure 9. Schematic Diagram Illustrating the Coordinated Regulation of *PHR1* by FHY3/FAR1, HY5, and EIN3/EIL1 in Response to Light and Ethylene Stimuli.

Three transcription factors (FHY3, HY5, and EIN3) converge on the *PHR1* promoter to coordinately regulate its expression. Light and ethylene act to promote *PHR1* expression and PSRs via promoting the accumulation of FHY3 and EIN3, two positive regulators of *PHR1* expression. Ethylene abrogates the repressive effect of HY5 on *PHR1* expression through blocking HY5 protein accumulation.

The "phosphorus problem" in sustainable agriculture systems has recently received much attention due to its limited supply and the damage to the ecosystem caused by its waste. It is highly desirable to breed crop plants with improved Pi acquisition efficiency or P use efficiency through biotechnology or molecular marker-assisted breeding, but such efforts have only met limited success thus far (Chiou and Lin, 2011; Baker et al., 2015). Recent studies have suggested that the regulatory pathway involving the activation of the expression of some genes by PHR1 in response to Pi starvation is likely conserved between monocotyledonous and dicotyledonous plants (Schünmann et al., 2004a, 2004b; K. Zhou et al., 2008). Overexpression of Arabidopsis *PHR1* and its homologs (maize [*Zea mays*], rice [*Oryza sativa*], oilseed rape [*Brassica napus*], and wheat [*Triticum aestivum*] *PHR1*) in transgenic plants led to enhanced root elongation, enhanced root hair growth, upregulation of several low-phosphate response genes, and improved Pi uptake. In some cases, the *PHR1*-overexpressing plants showed improved growth under low-Pi conditions (J. Wang et al., 2013; X. Wang et al., 2013; J. Zhou et al., 2008). Furthermore, PHR1 has emerged as a general regulator of phosphate, sulfate, zinc, and iron homeostasis in plants (Briat et al., 2015). The findings reported in this work may ultimately facilitate the design of crop cultivars with an improved ability to acquire and utilize Pi in the future.

METHODS

Plant Materials and Growth Conditions

The wild-type *Arabidopsis thaliana* plants used in this study were of the Col-0 ecotype unless otherwise indicated. The *fhy3-4*, *fhy3-4 far1-2*, *ProFHY3:FHY3-GR/fhy3-4*, and *ProFHY3:FHY3-YFP/fhy3-4* plants were in the No-0 ecotype background. The *phr1* T-DNA insertion mutant (SALK_067629C) was obtained from the Nottingham Arabidopsis Stock Centre. The *hy5 fhy3 far1* triple mutant was constructed by genetic crossing of the *hy5-215* and *fhy3-4 far1-2* mutants (Li et al., 2010). The *phyA-211*, *phyB-9*, *phyA phyB*, *phyABDE*, *phr1*, *ein3-1*, *ein3-1 eil1-1*, and estradiol-inducible *EIN3-FLAG* transgenic plants have been described previously (An et al., 2010; Li et al., 2011). The plant growth conditions were described previously (Cardona-López et al., 2015). For Pi+ medium, plants were grown in Murashige and Skoog (MS) medium supplemented with 1 mM KH_2PO_4. For Pi-deficient medium, KH_2PO_4 was replaced with equimolar amounts of KCl. Surface-sterilized seeds were sown on MS medium (2% sucrose and 0.75% agar, pH 5.8) and stratified at 4°C for 2 d. The plates were irradiated with white light (provided by full-spectrum white fluorescent light bulbs with a fluence rate of 200 μmol m^{-2} s^{-1}) for 10 h to promote germination and then incubated at 22°C under continuous white light or in darkness in a Percival growth chamber (Percival Scientific).

For chemical treatment, Arabidopsis seedlings were incubated in MS liquid medium supplemented with DEX (10 μM) or ACC (10 μM) before collection at the indicated time. In the mock solution, an equal volume of DMSO (0.1%) was added.

Plasmid Construction

All plasmids were constructed using an In-Fusion HD cloning kit (Clontech). To generate the *AtPHR1p:LacZ*, *AtPHR1p-I:LacZ*, *AtPHR1p-II:LacZ*, and *AtPHR1p-III:LacZ* reporter constructs, promoter regions were amplified and cloned into the *Eco*RI and *Xho*I sites of *pLaczi2μ* (Lin et al., 2007), respectively. For mutagenesis of the FBS, ACE, and EBS sites in the *PHR1* promoter, primers harboring mutation sites and overlapping with the *cis*-elements were used to amplify the *PHR1* promoter fragments containing the mutated *cis*-elements. The two PCR products were used as the templates for another round of overlapping PCR to obtain the mutated full-length *PHR1* promoter.

The JG-FHY3, LexA-FHY3, JG-FAR1, LexA-FAR1, and JG-HY5 constructs were described previously (Li et al., 2011). To generate the JG-EIN3 construct, the full-length coding sequence of EIN3 was amplified and cloned into the *Eco*RI/*Xho*I sites of the *pB42AD* vector. The GST-HY5 and GST-FHY3N recombinant fusion protein constructs were described previously (An et al., 2010; Li et al., 2010). To construct MBP-EIN3N (amino acids 141 to 352), the corresponding DNA fragment was PCR amplified and cloned into *pMAL-2c*. To prepare constructs for the BiFC assay, the full-length coding sequence (CDS) of EIN3 was cloned into the pSPYNE-35S vector digested with *Bam*HI/*Sal*I to generate EIN3-nYFP. The full-length CDS of FHY3 was cloned into the pSPYCE-35S vector digested with *Bam*HI/*Sal*I to generate FHY3-cYFP.

To generate constructs for the transient expression assay, the *PHR1* promoter was amplified and cloned into *pGreenII 0800-LUC* to give rise to *PHR1p:LUC*. The CDSs of FHY3, FAR1, and HY5 were amplified and cloned into *pSPYNE-35S* digested with *Bam*HI/*Sal*I to generate *Pro35S:FHY3*, *Pro35S:FAR1*, and *Pro35S:HY5*, respectively.

To generate *Pro35S:HY5-GFP*, the HY5 CDS was amplified and cloned into *pCambia1305* through the *Xba*I site. To generate *ProHY5:HY5-GR*, the GR steroid binding domain was PCR amplified and inserted into *pCambia1300* digested with *Hind*III to produce *pC1300-GR*. The genomic region of *HY5* was then amplified and inserted into *pC1300-GR* digested with *Sal*I. To generate *ProPHR1:GUS*, the *PHR1* promoter fragment was amplified and cloned into the PBI121 vector digested with *Sal*I, giving rise to *ProPHR1:GUS*.

Yeast Assays

For yeast one-hybrid assays, various plasmids of JG fusion proteins were cotransformed with the *ProPHR1:LacZ* reporter plasmid into yeast strain EGY48. For yeast two-hybrid assays, different combinations of JG and LexA fusion plasmids were cotransformed into yeast strain EGY48, which already harbors the *p8op:LacZ* reporter. Transformants were grown on proper drop-out plates containing 5-bromo-4-chloro-3-indolyl-β-D-galactopyranoside for blue color development.

Gene Expression Analysis via qRT-PCR

Total RNA was extracted from three biological replicates (~30 plants each) per sample using Trizol (Invitrogen), and the first-strand cDNA was synthesized from 1 μg of RNA using reverse transcriptase (Tiangen). The cDNA was diluted 1:10 and subjected to quantitative PCR using SuperReal PreMix Plus (Tiangen) and a 7500 Real Time PCR System (Applied Biosystems) cycler. Levels of *UBQ5* expression were used as the internal control. Primers are listed in Supplemental Table 1.

ChIP

Pro35S:FLAG-FHY3-HA (Li et al., 2011) and *pER8-EIN3-3FLAG* (An et al., 2010) transgenic seedlings were used in the ChIP assays. For the assay using *pER8-EIN3-3FLAG* transgenic seedlings, 7-d-old light-grown seedlings were transferred to MS liquid medium supplemented with 10 μM β-estradiol for 12 h and then harvested. For the HY5 ChIP assay, rabbit anti-HY5 antibodies (Li et al., 2010) were used. The procedure used for ChIP has been described previously (Lin et al., 2007). Briefly, ~2 g of seedlings grown under the indicated conditions was cross-linked with 1% formaldehyde under a vacuum. The chromatin complexes were isolated and incubated with specific antibodies overnight. The precipitated DNA was recovered and analyzed by qPCR using the primers listed in Supplemental Table 1.

EMSA

EMSA was performed using a LightShift Chemiluminescent EMSA kit (Pierce) according to the manufacturer's instructions. The oligonucleotide sequences of biotin-labeled and unlabeled probes are listed in Supplemental Table 1. The GST-FHY3N, GST-HY5, and MBP-EIN3N fusion proteins were expressed in *Escherichia coli* strain BL21. The recombinant proteins were purified using either GST-agarose or amylose resin affinity chromatography. Briefly, synthetic DNA oligonucleotide probes labeled with biotin were incubated with the recombinant proteins in the presence or absence of excess amounts of unlabeled competitors for 20 min at room temperature. The DNA-protein complexes were separated on 6% native polyacrylamide gels. For the competition assays, 1, 2, and 4 μg of GST-HY5 were used to compete with 2 μg of GST-FHY3N.

Immunoprecipitation Assay

For coimmunoprecipitation, total proteins were homogenized in extraction buffer (50 mM Tris-HCl, pH 7.5, 150 mM NaCl, 10 mM $MgCl_2$, 0.1% Tween 20, 1 mM PMSF, 1× complete protease inhibitor cocktail [Roche]) and centrifuged at 12,000*g* two times. Cleared extract was combined with anti-HA magnetic agarose beads (MBL) and incubated for 6 h at 4°C. After washing five times with coimmunoprecipitation washing buffer (100 mM NaCl and 20 mM Tris-HCl, pH 7.6), the magnetic agarose was resuspended in extraction buffer. For immunoblot analysis, samples were separated by SDS-PAGE, and the target protein was detected with anti-FLAG (1:4000) or anti-HA (1:5000) antibody (MBL; M185-7 or M180-7, respectively). The secondary antibody used is HRP-conjugate (MBL; 1:8000).

LCI Assays

The firefly LCI assays were performed using *Nicotiana benthamiana* leaves. Full-length EIN3 was fused to N-terminal luciferase (nLUC), and FHY3 was fused to C-terminal LUC (cLUC). Both the nLUC- and cLUC-fused proteins were coinfiltrated into *N. benthamiana* leaves via *Agrobacterium tumefaciens*-mediated coinfiltration. The infiltrated plants were incubated under continuous light or darkness for 3 d before examining using the NightSHADE LB 985 Plant Imaging System (Berthold).

Transient Expression Assay

Transient expression assays were performed as described previously (Li et al., 2011). The reporter and effector constructs were transformed into Agrobacterium strain EHA105. The Agrobacterium solutions containing the reporter or effector constructs were coincubated for 2 h and infiltrated into 3- to 4-week-old *N. benthamiana* leaves. Plants were incubated under continuous white light for 3 d after infiltration. The firefly LUC activity was photographed after spraying with 1 mM luciferin (Goldbio). For the dual-luciferase quantification assay, firefly luciferase and *Renilla* luciferase activities were assayed as described previously (Li et al., 2010).

Confocal Microscopy

GFP and YFP signals in transgenic plants were observed in roots by confocal microscopy (Zeiss LSM 710) with the argon laser at 488-nm excitation and band-pass filter at 500- to 530-nm emission. Levels of fluorescence in the nuclei were calculated using ImageJ. For 4′,6-diamidino-2-phenylindole staining, fluorescence was observed under excitation at 405 nm and emission at 474 to 525 nm.

Pi and Anthocyanin Measurements

For total Pi content measurement, the method of Ames (1966) was used. Anthocyanin contents were measured as described previously (Swain and Hillis, 1959). For the primary root length measurement, plants were grown on vertical MS plates (+Pi, −Pi, +ACC, or +$AgNO_3$) for 10 d before being photographed under a dissecting microscope with a camera (Canon E05 60D) and analyzed using ImageJ.

GO Enrichment Analysis

GO enrichment for FHY3, HY5, and EIN3 coregulated genes was performed using AgriGO (http://bioinfo.cau.edu.cn/agriGO/). Enrichment was determined by the Fisher method with a multiple testing correction based on a Hochberg false discovery rate cutoff of 0.05.

Accession Numbers

Sequence data from this article can be found in the GenBank/EMBL libraries under the following accession numbers: PHR1 (At4g28610), FHY3 (At3g22170), FAR1 (At4g15090), HY5 (At5g11260), EIN3 (At3g20770), EIL1 (At2g27050), ACP5 (At3g17790), PHF1 (At3g52190), PMH1 (At3g22310), IPS1 (At3g09922), PRE8 (At4g14090), RNS1 (At2g02990), SPX1 (At5g20150), SQD1 (At4g33030), TMT1 (At2g43920), PHYA (At1g09570), PHYB (At2g18790), PHYD (At4g16250), and PHYE (At4g18130).

Supplemental Data

Supplemental Figure 1. PSI Gene Expression and Anthocyanin Content Measurement.

Supplemental Figure 2. Histograms Showing Pi Content in Wild-Type (Col-0 and No-0), *phyA-211*, *phyB-9*, *phyA phyB*, *phyABDE*, *fhy3-4*, *fhy3-4 far1-2*, *hy5-215*, *ein3-1*, and *ein3-1 eil1-1* Mutant Plants.

Supplemental Figure 3. PSI Gene Expression and Anthocyanin Content Measurement in *fhy3-4 far1-2* and *hy5-215* Mutants.

Supplemental Figure 4. Genetic Interaction Analysis of FHY3/FAR1, HY5, EIN3, and PHR1.

Supplemental Figure 5. FHY3 and HY5 Regulate *PHR1* Expression.

Supplemental Figure 6. Primary Root Length in Wild-Type (Col-0 and No-0), *phr1*, *fhy3-4*, *fhy3-4 far1-2*, and *hy5-215* Mutant Plants.

Supplemental Figure 7. qRT-PCR Analysis of PSI Gene Expression in the *ein3-1 eil1-1* Mutant.

Supplemental Figure 8. EIN3 Regulates *PHR1* Expression.

Supplemental Figure 9. qRT-PCR Analysis of PSI Gene (*SPX1* and *PHF1*) Expression.

Supplemental Figure 10. LCI Assay Showing EIN3 and FHY3 Interaction.

Supplemental Figure 11. Venn Diagrams and GO Analysis of FHY3, HY5, and EIN3 Coregulated Genes.

Supplemental Table 1. Primer Sets Used in This Study.

Supplemental Data Set 1. List of EIN3, FHY3, and HY5 Coregulated Genes.

ACKNOWLEDGMENTS

We thank Dr. Shangwei Zhong of Peking University for providing us with seeds of *ein3-1* and *ein3-1 eil1-1* mutants and estradiol-inducible *EIN3-FLAG* transgenic plants. This work was supported by funds from the National Natural Science Foundation of China (Grants 31430008 and 31500239).

AUTHOR CONTRIBUTIONS

H.Y.W. and Y.L. designed research. Y.L., Y.X., X.M., and W.Y. performed research. Y.L., Y.X., H.W., and H.Y.W. analyzed data. H.Y.W. and Y.L. wrote the article.

Received April 4, 2017; revised August 8, 2017; accepted August 24, 2017; published August 25, 2017.

REFERENCES

Ames, B.N. (1966). Assay of inorganic phosphate, total phosphate and phosphatases. Methods Enzymol. **8:** 115–118.

An, F., et al. (2010). Ethylene-induced stabilization of ETHYLENE INSENSITIVE3 and EIN3-LIKE1 is mediated by proteasomal degradation of EIN3 binding F-box 1 and 2 that requires EIN2 in *Arabidopsis*. Plant Cell **22:** 2384–2401.

Baker, A., Ceasar, S.A., Palmer, A.J., Paterson, J.B., Qi, W., Muench, S.P., and Baldwin, S.A. (2015). Replace, reuse, recycle: improving the sustainable use of phosphorus by plants. J. Exp. Bot. **66:** 3523–3540.

Bari, R., Datt Pant, B., Stitt, M., and Scheible, W.R. (2006). PHO2, microRNA399, and PHR1 define a phosphate-signaling pathway in plants. Plant Physiol. **141:** 988–999.

Bariola, P.A., Howard, C.J., Taylor, C.B., Verburg, M.T., Jaglan, V.D., and Green, P.J. (1994). The *Arabidopsis* ribonuclease gene RSN1 is tightly controlled in response to phosphate limitation. Plant J. **6:** 673–685.

Basu, P., Zhang, Y.J., Lynch, J.P., and Brown, K.M. (2007). Ethylene modulates genetic, positional, and nutritional regulation of root plagiogravitropism. Funct. Plant Biol. **34:** 41–51.

Briat, J.F., Rouached, H., Tissot, N., Gaymard, F., and Dubos, C. (2015). Integration of P, S, Fe, and Zn nutrition signals in *Arabidopsis thaliana*: potential involvement of PHOSPHATE STARVATION RESPONSE 1 (PHR1). Front. Plant Sci. **6:** 290.

Bustos, R., Castrillo, G., Linhares, F., Puga, M.I., Rubio, V., Pérez-Pérez, J., Solano, R., Leyva, A., and Paz-Ares, J. (2010). A central regulatory system largely controls transcriptional activation and repression responses to phosphate starvation in *Arabidopsis*. PLoS Genet. **6:** e1001102.

Cardona-López, X., Cuyas, L., Marín, E., Rajulu, C., Irigoyen, M.L., Gil, E., Puga, M.I., Bligny, R., Nussaume, L., Geldner, N., Paz-Ares, J., and Rubio, V. (2015). ESCRT-III-associated protein ALIX mediates high affinity phosphate transporter trafficking to maintain phosphate homeostasis in *Arabidopsis*. Plant Cell **27:** 2560–2581.

Chang, K.N., et al. (2013). Temporal transcriptional response to ethylene gas drives growth hormone cross-regulation in *Arabidopsis*. eLife **2:** e00675.

Chen, M., Chory, J., and Fankhauser, C. (2004). Light signal transduction in higher plants. Annu. Rev. Genet. **38:** 87–117.

Chiou, T.J., and Lin, S.I. (2011). Signaling network in sensing phosphate availability in plants. Annu. Rev. Plant Biol. **62:** 185–206.

Delhaize, E., and Randall, P.J. (1995). Characterization of a phosphate-accumulator mutant of *Arabidopsis thaliana*. Plant Physiol. **107:** 207–213.

Franco-Zorrilla, J.M., Martín, A.C., Leyva, A., and Paz-Ares, J. (2005). Interaction between phosphate-starvation, sugar, and cytokinin signaling in Arabidopsis and the roles of cytokinin receptors CRE1/AHK4 and AHK3. Plant Physiol. **138:** 847–857.

Guo, H., and Ecker, J.R. (2003). Plant responses to ethylene gas are mediated by SCF(EBF1/EBF2)-dependent proteolysis of EIN3 transcription factor. Cell **115:** 667–677.

He, C.J., Morgan, P.W., and Drew, M.C. (1992). Enhanced sensitivity to ethylene in nitrogen-or phosphate-starved roots of *Zea mays* L. during aerenchyma formation. Plant Physiol. **98:** 137–142.

Huang, X., Ouyang, X., Yang, P., Lau, O.S., Li, G., Li, J., Chen, H., and Deng, X.W. (2012). *Arabidopsis* FHY3 and HY5 positively mediate induction of COP1 transcription in response to photomorphogenic UV-B light. Plant Cell **24:** 4590–4606.

Hudson, M., Ringli, C., Boylan, M.T., and Quail, P.H. (1999). The FAR1 locus encodes a novel nuclear protein specific to phytochrome A signaling. Genes Dev. **13:** 2017–2027.

Jain, A., Poling, M.D., Karthikeyan, A.S., Blakeslee, J.J., Peer, W.A., Titapiwatanakun, B., Murphy, A.S., and Raghothama, K.G. (2007). Differential effects of sucrose and auxin on localized phosphate deficiency-induced modulation of different traits of root system architecture in Arabidopsis. Plant Physiol. **144:** 232–247.

Jiang, C., Gao, X., Liao, L., Harberd, N.P., and Fu, X. (2007). Phosphate starvation root architecture and anthocyanin accumulation responses are modulated by the gibberellin-DELLA signaling pathway in Arabidopsis. Plant Physiol. **145:** 1460–1470.

Jing, Y., Zhang, D., Wang, X., Tang, W., Wang, W., Huai, J., Xu, G., Chen, D., Li, Y., and Lin, R. (2013). Arabidopsis chromatin remodeling factor PICKLE interacts with transcription factor HY5 to regulate hypocotyl cell elongation. Plant Cell **25:** 242–256.

Karthikeyan, A.S., Varadarajan, D.K., Jain, A., Held, M.A., Carpita, N.C., and Raghothama, K.G. (2007). Phosphate starvation responses are mediated by sugar signaling in *Arabidopsis*. Planta **225:** 907–918.

Kim, H.J., Lynch, J.P., and Brown, K.M. (2008). Ethylene insensitivity impedes a subset of responses to phosphorus deficiency in tomato and petunia. Plant Cell Environ. **31:** 1744–1755.

Klecker, M., Gasch, P., Peisker, H., Dörmann, P., Schlicke, H., Grimm, B., and Mustroph, A. (2014). A shoot-specific hypoxic response of Arabidopsis sheds light on the role of the phosphate-responsive transcription factor PHOSPHATE STARVATION RESPONSE1. Plant Physiol. **165:** 774–790.

Lee, J., He, K., Stolc, V., Lee, H., Figueroa, P., Gao, Y., Tongprasit, W., Zhao, H., Lee, I., and Deng, X.W. (2007). Analysis of transcription factor HY5 genomic binding sites revealed its hierarchical role in light regulation of development. Plant Cell **19:** 731–749.

Lei, M., Liu, Y., Zhang, B., Zhao, Y., Wang, X., Zhou, Y., Raghothama, K.G., and Liu, D. (2011a). Genetic and genomic evidence that sucrose is a global regulator of plant responses to phosphate starvation in Arabidopsis. Plant Physiol. **156:** 1116–1130.

Lei, M., Zhu, C., Liu, Y., Karthikeyan, A.S., Bressan, R.A., Raghothama, K.G., and Liu, D. (2011b). Ethylene signaling is involved in regulation of phosphate starvation-induced gene expression and production of acid phosphatases and anthocyanin in *Arabidopsis*. New Phytol. **189:** 1084–1095.

Li, G., et al. (2011). Coordinated transcriptional regulation underlying the circadian clock in *Arabidopsis*. Nat. Cell Biol. **13:** 616–622.

Li, J., Li, G., Gao, S., Martinez, C., He, G., Zhou, Z., Huang, X., Lee, J.H., Zhang, H., Shen, Y., Wang, H., and Deng, X.W. (2010). *Arabidopsis* transcription factor ELONGATED HYPOCOTYL5 plays a role in the feedback regulation of phytochrome A signaling. Plant Cell **22:** 3634–3649.

Li, Y.S., Mao, X.T., Tian, Q.Y., Li, L.H., and Zhang, W.H. (2009). Phosphorus deficiency-induced reduction in root hydraulic conductivity in *Medicago falcata* is associated with ethylene production. Environ. Exp. Bot. **67:** 172–177.

Lin, R., Ding, L., Casola, C., Ripoll, D.R., Feschotte, C., and Wang, H. (2007). Transposase-derived transcription factors regulate light signaling in *Arabidopsis*. Science **318:** 1302–1305.

Liu, J., Samac, D.A., Bucciarelli, B., Allan, D.L., and Vance, C.P. (2005). Signaling of phosphorus deficiency-induced gene expression in white lupin requires sugar and phloem transport. Plant J. **41:** 257–268.

Liu, J.Q., Allan, D.L., and Vance, C.P. (2010). Systemic signaling and local sensing of phosphate in common bean: cross-talk between photosynthate and microRNA399. Mol. Plant **3:** 428–437.

López-Arredondo, D.L., Leyva-González, M.A., González-Morales, S.I., López-Bucio, J., and Herrera-Estrella, L. (2014). Phosphate nutrition: improving low-phosphate tolerance in crops. Annu. Rev. Plant Biol. **65:** 95–123.

López-Bucio, J., Cruz-Ramírez, A., and Herrera-Estrella, L. (2003). The role of nutrient availability in regulating root architecture. Curr. Opin. Plant Biol. **6:** 280–287.

Marschner, H. (1995). Mineral Nutrition of Higher Plants. (San Diego, CA: Academic Press).

Martín, A.C., del Pozo, J.C., Iglesias, J., Rubio, V., Solano, R., de La Peña, A., Leyva, A., and Paz-Ares, J. (2000). Influence of cytokinins on the expression of phosphate starvation responsive genes in *Arabidopsis*. Plant J. **24:** 559–567.

Misson, J., et al. (2005). A genome-wide transcriptional analysis using *Arabidopsis thaliana* Affymetrix gene chips determined plant responses to phosphate deprivation. Proc. Natl. Acad. Sci. USA **102:** 11934–11939.

Miura, K., Rus, A., Sharkhuu, A., Yokoi, S., Karthikeyan, A.S., Raghothama, K.G., Baek, D., Koo, Y.D., Jin, J.B., Bressan, R.A., Yun, D.J., and Hasegawa, P.M. (2005). The *Arabidopsis* SUMO E3 ligase SIZ1 controls phosphate deficiency responses. Proc. Natl. Acad. Sci. USA **102:** 7760–7765.

Morcuende, R., Bari, R., Gibon, Y., Zheng, W., Pant, B.D., Bläsing, O., Usadel, B., Czechowski, T., Udvardi, M.K., Stitt, M., and Scheible, W.R. (2007). Genome-wide reprogramming of metabolism and regulatory networks of *Arabidopsis* in response to phosphorus. Plant Cell Environ. **30:** 85–112.

Nagarajan, V.K., and Smith, A.P. (2012). Ethylene's role in phosphate starvation signaling: more than just a root growth regulator. Plant Cell Physiol. **53:** 277–286.

Nilsson, L., Müller, R., and Nielsen, T.H. (2007). Increased expression of the MYB-related transcription factor, *PHR1*, leads to enhanced phosphate uptake in *Arabidopsis thaliana*. Plant Cell Environ. **30:** 1499–1512.

Osterlund, M.T., Hardtke, C.S., Wei, N., and Deng, X.W. (2000). Targeted destabilization of HY5 during light-regulated development of *Arabidopsis*. Nature **405:** 462–466.

Ouyang, X., et al. (2011). Genome-wide binding site analysis of FAR-RED ELONGATED HYPOCOTYL3 reveals its novel function in *Arabidopsis* development. Plant Cell **23:** 2514–2535.

Poirier, Y., Thoma, S., Somerville, C., and Schiefelbein, J. (1991). Mutant of Arabidopsis deficient in xylem loading of phosphate. Plant Physiol. **97:** 1087–1093.

Puga, M.I., et al. (2014). SPX1 is a phosphate-dependent inhibitor of PHOSPHATE STARVATION RESPONSE 1 in *Arabidopsis*. Proc. Natl. Acad. Sci. USA **111:** 14947–14952.

Raghothama, K.G. (1999). Phosphate acquisition. Annu. Rev. Plant Physiol. Plant Mol. Biol. **50:** 665–693.

Rubio, V., Linhares, F., Solano, R., Martín, A.C., Iglesias, J., Leyva, A., and Paz-Ares, J. (2001). A conserved MYB transcription factor involved in phosphate starvation signaling both in vascular plants and in unicellular algae. Genes Dev. **15:** 2122–2133.

Schünmann, P.H., Richardson, A.E., Smith, F.W., and Delhaize, E. (2004a). Characterization of promoter expression patterns derived from the Pht1 phosphate transporter genes of barley (*Hordeum vulgare* L.). J. Exp. Bot. **55:** 855–865.

Schünmann, P.H., Richardson, A.E., Vickers, C.E., and Delhaize, E. (2004b). Promoter analysis of the barley Pht1;1 phosphate transporter gene identifies regions controlling root expression and responsiveness to phosphate deprivation. Plant Physiol. **136:** 4205–4214.

Shi, H., Shen, X., Liu, R., Xue, C., Wei, N., Deng, X.W., and Zhong, S. (2016). The red light receptor phytochrome B directly enhances substrate-E3 ligase interactions to attenuate ethylene responses. Dev. Cell **39:** 597–610.

Siddiqui, H., Khan, S., Rhodes, B.M., and Devlin, P.F. (2016). FHY3 and FAR1 act downstream of light stable phytochromes. Front. Plant Sci. **7:** 175.

Solano, R., Stepanova, A., Chao, Q.M., and Ecker, J.R. (1998). Nuclear events in ethylene signaling: a transcriptional cascade mediated by ETHYLENE-INSENSITIVE3 and ETHYLENE-RESPONSE-FACTOR1. Genes Dev. **12:** 3703–3714.

Song, L., and Liu, D. (2015). Ethylene and plant responses to phosphate deficiency. Front. Plant Sci. **6:** 796.

Song, L., Yu, H., Dong, J., Che, X., Jiao, Y., and Liu, D. (2016). The molecular mechanism of ethylene-mediated root hair development induced by phosphate starvation. PLoS Genet. **12:** e1006194.

Swain, T., and Hillis, W. (1959). Phenolic constituents of *Prunus domestica*. I. Quantitative analysis of phenolic constituents. J. Sci. Food Agric. **10:** 63–68.

Thibaud, M.C., Arrighi, J.F., Bayle, V., Chiarenza, S., Creff, A., Bustos, R., Paz-Ares, J., Poirier, Y., and Nussaume, L. (2010). Dissection of local and systemic transcriptional responses to phosphate starvation in *Arabidopsis*. Plant J. **64:** 775–789.

Wang, H., and Deng, X.W. (2002). *Arabidopsis* FHY3 defines a key phytochrome A signaling component directly interacting with its homologous partner FAR1. EMBO J. **21:** 1339–1349.

Wang, H., and Wang, H. (2015). Multifaceted roles of FHY3 and FAR1 in light signaling and beyond. Trends Plant Sci. **20:** 453–461.

Wang, J., Sun, J., Miao, J., Guo, J., Shi, Z., He, M., Chen, Y., Zhao, X., Li, B., Han, F., Tong, Y., and Li, Z. (2013). A phosphate starvation response regulator Ta-PHR1 is involved in phosphate signaling and increases grain yield in wheat. Ann. Bot. (Lond.) **111:** 1139–1153.

Wang, K.L., Yoshida, H., Lurin, C., and Ecker, J.R. (2004). Regulation of ethylene gas biosynthesis by the *Arabidopsis* ETO1 protein. Nature **428:** 945–950.

Wang, L., Dong, J., Gao, Z., and Liu, D. (2012). The *Arabidopsis* gene HYPERSENSITIVE TO PHOSPHATE STARVATION3 encodes ETHYLENE OVERPRODUCTION1. Plant Cell Physiol. **53:** 1093–1105.

Wang, X., Bai, J., Liu, H., Sun, Y., Shi, X., and Ren, Z. (2013). Overexpression of a maize transcription factor ZmPHR1 improves shoot inorganic phosphate content and growth of *Arabidopsis* under low-phosphate conditions. Plant Mol. Biol. Rep. **31:** 665–677.

Yu, Y., Wang, J., Zhang, Z., Quan, R., Zhang, H., Deng, X.W., Ma, L., and Huang, R. (2013). Ethylene promotes hypocotyl growth and HY5 degradation by enhancing the movement of COP1 to the nucleus in the light. PLoS Genet. **9:** e1004025.

Zhang, H., He, H., Wang, X., Wang, X., Yang, X., Li, L., and Deng, X.W. (2011). Genome-wide mapping of the HY5-mediated gene networks in *Arabidopsis* that involve both transcriptional and post-transcriptional regulation. Plant J. **65:** 346–358.

Zhang, Z., Liao, H., and Lucas, W.J. (2014). Molecular mechanisms underlying phosphate sensing, signaling, and adaptation in plants. J. Integr. Plant Biol. **56:** 192–220.

Zhong, S., Shi, H., Xue, C., Wei, N., Guo, H., and Deng, X.W. (2014). Ethylene-orchestrated circuitry coordinates a seedling's response to soil cover and etiolated growth. Proc. Natl. Acad. Sci. USA **111:** 3913–3920.

Zhou, J., Jiao, F., Wu, Z., Li, Y., Wang, X., He, X., Zhong, W., and Wu, P. (2008). OsPHR2 is involved in phosphate-starvation signaling and excessive phosphate accumulation in shoots of plants. Plant Physiol. **146:** 1673–1686.

Zhou, K., Yamagishi, M., Osaki, M., and Masuda, K. (2008). Sugar signaling mediates cluster root formation and phosphorus starvation-induced gene expression in white lupin. J. Exp. Bot. **59:** 2749–2756.

Zhu, Z., et al. (2011). Derepression of ethylene-stabilized transcription factors (EIN3/EIL1) mediates ethylene signaling synergy in *Arabidopsis*. Proc. Natl. Acad. Sci. USA **108:** 12539–12544.